Lateral photon transport in dense scattering and weakly absorbing media of finite thickness: asymptotic analysis of the space–time Green function

Igor N. Polonsky and Anthony B. Davis

Los Alamos National Laboratory, Space and Remote Sensing Sciences Group (ISR-2), Los Alamos, New Mexico 87545-0000

Received October 6, 2003; revised manuscript received January 20, 2004; accepted January 23, 2004

The asymptotic law for the radial distribution of radiance density from an isotropic point source placed in a slab of homogeneous absorbing and scattering material is obtained within the framework of diffusion theory. The exponential shape of the tail of the resulting Green function has been observed but was not theoretically explained until now. We derive formulas for both the steady-state and the time-dependent problems. The theoretical results are verified by comparison with Monte Carlo simulations. © 2004 Optical Society of America

OCIS codes: 000.3860, 010.1300, 170.3660.

1. INTRODUCTION AND OUTLINE

Measurement of the characteristics of the reflected and transmitted radiance is a widely used approach to obtaining information remotely about a scattering medium in applications ranging from geophysics to medicine. This technique can provide excellent time resolution (we can have a series of snapshots to study a given medium) and–or spatial coverage (if using a moving platform such as a satellite or aircraft). However, the physical information content derived from a particular technique depends on what model of the radiance propagation is employed. In particular, the single-scattering model, along with minor corrections for multiple-scattering effects, is sufficient for atmospheric aerosol sounding of either transmitted solar radiance [the AERONET (Aerosol Robotic Network)[1]] or its reflected counterpart (satellite-based passive sensors). In contrast, tissue optics,[2–5] as well as sounding of clouds[6,7] and of seawater,[8,9] must include multiple-scattering effects to retrieve information about the scattering medium. In fact, multiply scattered photons dominate the signal.

Accounting for multiple scattering generally means that the radiative transfer equation,[10] often with time dependence,[11] has to be solved while assuming the appropriate boundary and initial conditions. This can become an insurmountable problem, as solution of the corresponding three-dimensional (3D) time-dependent radiation transfer equation may require significant computer time, which is not acceptable if real-time retrieval procedures and–or analysis are required. Fortunately, a number of approximations have been developed which provide efficient and reasonably accurate solutions of the radiative transfer equation if some necessary conditions are fulfilled. For the case of optically dense, weakly absorbing media, such as water-droplet clouds in atmospheric optics or biological tissue in medicine, both of which are of particular interest to us, the framework of the diffusion approximation[12] (DA) can be used. The simplicity of this approach allows one to derive an analytical solution for the forward problems, such as image transfer,[13] simulation of radiance characteristics in 3D cloud optics,[14,15] and those in tissue optics.[2–5] Moreover, the analytical relationships obtained within the DA make it possible to solve inverse problems.[16–19]

The use of the DA to calculate the spatial and temporal characteristics of the radiance field is a well-developed area.[2–7,13,20] However, the final expressions do not have a simple form, even if we are interested only in the asymptotic behavior of a given characteristic. For example, it appears that the question, "What is the law for the asymptotic behavior of radiance at large distance from the point of incidence?" still has not been answered in a simple way, beyond the case of a semi-infinite medium. The only available option is to use formulas[5,13,20] with an infinite sum of terms, but this technique has the disadvantage of slow convergence and, more disappointing, it does not provide us with an asymptotic law.

Why is the asymptotic law important and is there any practical use of it? In medical optics asymptotic results for the semi-infinite medium have successfully been employed to retrieve information about tissue optical properties.[21,22] Formulas for the semi-infinite slab have thus been used for finite size media, and this can be justified by the very large values of the extinction coefficient (very small mean free path) in the biological tissue.[22,23] However, this is not generally the case for cloud optics; otherwise, it would be impossible to retrieve a cloud optical thickness by using the appropriate asymptotic formulas.[24] Moreover, the radial distribution of radiance characterizes the process of horizontal photon transport,

which limits the use of the so-called independent pixel approximation (IPA)[25] and results in the scale-break phenomenon[26] observed in high-resolution satellite images of extensive clouds. Knowledge of the asymptotic law is needed to gain further insight into this phenomenon.

The goal of this work is to identify and express in closed form the asymptotic behavior of the spatial radiance characteristics in the case of a homogenous slab of finite thickness illuminated from an internal or boundary point. In the framework of linear transport theory, which is ideally where we want to work, this Green-function problem has been addressed analytically only for the semi-infinite, isotropically scattering medium,[27] or by a method of successive refinements that starts with an exponential ansatz.[28] So we will benchmark our exact results in the DA against purely numerical solutions of the associated radiative transfer problem obtained by a robust Monte Carlo technique.

The structure of the paper is as follows. In Section 2 the derivation of the asymptotic behavior by use of the DA is given. The accuracy of the formula we obtained is tested by comparison with Monte Carlo simulations in Section 3. We discuss some ramifications for cloud remote sensing and other optical diagnostics in Section 4. Finally, we summarize and trace the direction of further studies in Section 5.

2. ASYMPTOTICS OF GREEN FUNCTIONS OF RADIATIVE TRANSFER

A. Green Functions in the Diffusion Approximation

For the sake of simplicity let us consider a homogeneous slab of geometrical thickness H illuminated by a δ pulse from an internal or boundary point source, which we will assume to be isotropic. We will use the Cartesian coordinate system with z as the axis directed along an inner normal to the lower boundary that also contains the origin; in this way our source has coordinates $(0, 0, z_0)$ with $0 \leqslant z_0 \leqslant H$. We will use bold symbols for ordinary 3D vectors, and we will employ symbols with an arrow above to denote two-dimensional vectors that are the projections of the 3D vectors on the plane xOy. The mathematical model of this process may be developed within the DA,[12] which is based on the assumption that the radiance $I(t, \vec{r}, z, \mathbf{n})$ at point $\mathbf{x} = (\vec{r}, z)$ and time t in direction $\mathbf{n}$ (a unitary 3D vector) can be represented as

$$I(t, \vec{r}, z, \mathbf{n}) = \frac{1}{4\pi}[J(t, \vec{r}, z) + 3\mathbf{n} \cdot \mathbf{F}(t, \vec{r}, z)], \quad (1)$$

where

$$J(t, \vec{r}, z) = \int_{4\pi} I(t, \vec{r}, z, \mathbf{n}) \mathrm{d}\mathbf{n}, \quad (2)$$

$$\mathbf{F}(t, \vec{r}, z) = \int_{4\pi} \mathbf{n} I(t, \vec{r}, z, \mathbf{n}) \mathrm{d}\mathbf{n}. \quad (3)$$

The goal of the DA is to replace the standard integrodifferential transport equation that is obeyed by $I(t, \vec{r}, z, \mathbf{n})$ with simpler equations for $J(t, \vec{r}, z)$ and $\mathbf{F}(t, \vec{r}, z)$.

The most elegant derivation of DA equations from the radiative transfer equation is based on asymptotic theory.[29] The DA quantities $J(t, \vec{r}, z)$ and $\mathbf{F}(t, \vec{r}, z)$ satisfy the so-called telegrapher's system of coupled partial differential equations[30]

$$\frac{1}{c}\frac{\partial J}{\partial t} + \nabla \cdot \mathbf{F} + (\sigma_e - \sigma_s) J(t, \vec{r}, z) = E_0 \delta(t) \delta(\vec{r}) \delta(z - z_0), \quad (4a)$$

$$\frac{1}{c}\frac{\partial \mathbf{F}}{\partial t} + \frac{1}{3}\nabla J + (\sigma_e - \sigma_s g)\mathbf{F}(t, \vec{r}, z) = 0. \quad (4b)$$

Here c is the speed of light; σ_e and σ_s are the constant extinction and scattering coefficients, respectively; g is the asymmetry parameter of the medium's phase function (mean cosine of the scattering angle); and E_0 is the total energy of the pulsed point source of interest here. The gradient operator ∇ applies to the 3D position vector $\mathbf{x} = (\vec{r}, z)$.

Equation (4a) is the local expression of radiant energy conservation by advection ($c^{-1}\partial J/\partial t + \nabla \cdot \mathbf{F}$), its rate of destruction by absorption ($\sigma_a J$, where $\sigma_a = \sigma_e - \sigma_s$ is the absorption coefficient), and its rate of creation (right-hand side, in this case by a δ source). This is exact whether or not Eq. (1) holds as an expression for radiance. Equation (4b), on the other hand, is approximate and follows directly from Eq. (1) when it is substituted into the radiative transfer equation. Fick's law of diffusion, $\mathbf{F} = -D\nabla U$, where $U = J/c$ is radiant energy density, follows from Eq. (4b) by further neglecting $\partial \mathbf{F}/\partial t$ and recognizing

$$D = \frac{c}{3(\sigma_e - \sigma_s g)} = \frac{c l_t}{3} \quad (5)$$

as the diffusivity constant, where $l_t = 1/(\sigma_e - \sigma_s g)$ is the transport mean free path. In boundary-free space, a classic exercise shows that $\langle \mathbf{x}^2 \rangle = Dt$, where $\langle \cdot \rangle$ means a spatial average over photon density $J(t, \mathbf{x})$.

We start by introducing the dimensionless variables

$$u = \sigma_e c t, \quad (6a)$$

$$\vec{\rho} = \sigma_e \vec{r}, \quad (6b)$$

$$\tau = \sigma_e z, \quad (6c)$$

the last quantity being optical depth (hence, $\tau_0 = \sigma_e z_0$ for the source depth). Then we take a Laplace transform with respect to u and a Fourier transform with respect to the radial coordinates $\vec{\rho}$:

$$f(s) = \int_0^\infty \exp(-su) f(u) \mathrm{d}u, \quad (7)$$

$$f(\vec{k}) = \int^{+\infty} \int_{-\infty} \exp(-i\vec{k} \cdot \vec{\rho}) f(\vec{\rho}) \mathrm{d}\vec{\rho}. \quad (8)$$

Any confusion from using the same symbols for the original and transformed quantity will be avoided by writing

out the argument explicitly. As a result, we arrive at the system of coupled ordinary differential equations

$$\mathbf{F}(s, \vec{k}, \tau) = -\frac{1}{3(1 + s - \varpi_0 g)}\left(iJ\vec{k}, \frac{\mathrm{d}J}{\mathrm{d}\tau}\right), \tag{9a}$$

$$\frac{\mathrm{d}^2 J}{\mathrm{d}\tau^2} - m^2 J(s, \vec{k}, \tau) = -3c\sigma_e{}^3 E_0(1 + s - \varpi_0 g)\delta(\tau - \tau_0). \tag{9b}$$

Here $\varpi_0 = \sigma_s/\sigma_e$ is the single-scattering albedo, and

$$m = [k^2 + 3(1 + s - \varpi_0)(1 + s - \varpi_0 g)]^{1/2}. \tag{10}$$

This is a generalization of the diffusion constant $[3(1 - \varpi_0)(1 - \varpi_0 g)]^{1/2}$ used for the standard problem of horizontally uniform ($k = 0$) and steady ($s = 0$) illumination.

Boundary conditions for the DA are of the Robin (or "mixed") type,

$$\left[1 - \chi\frac{\partial}{\partial\tau}\right]J(s, \vec{k}, \tau)|_{\tau=0} = 0, \tag{11a}$$

$$\left[1 + \chi\frac{\partial}{\partial\tau}\right]J(s, \vec{k}, \tau)|_{\tau=\tau_H} = 0, \tag{11b}$$

where $\tau_H = \sigma_e H$ is the optical thickness of the slab and χ is the "extrapolation" length[12,30] in optical units. The definition of χ is discussed for problems in atmospheric optics by Davis and Marshak[15] and in biological tissue optics by Contini *et al.*[5] In our work, we will assume that

$$\chi = \frac{2/3}{(1 + s - \varpi_0 g)}, \tag{12}$$

while acknowledging that the choice of 2/3 in the numerator can be adjusted slightly for the sake of better reproducing numerical simulation results as shown by Davison,[12] Davis and Marshak,[15] and others.

Following Davison,[12] we will assume more tractable boundary conditions in the form

$$J(s, \vec{k}, \tau = -\chi) = 0, \tag{13a}$$

$$J(s, \vec{k}, \tau = \tau_H + \chi) = 0. \tag{13b}$$

So we are effectively solving the diffusive transport problem in a somewhat larger domain than the optical medium *per se*, which is for $0 < \tau < \tau_H$. Here as in conditions (11) we are expressing that there is no incoming flux at the lower ($\tau = 0$) and upper ($\tau = \tau_H$) boundaries of the medium.

The solution of Eq. (9b) with conditions (13) is

$$J(s, \vec{k}, \tau) = c\sigma_e{}^3 E_0 \frac{\cosh[m(\tau_H + 2\chi - |\tau - \tau_0|)] - \cosh\{m[\tau_H - (\tau + \tau_0)]\}}{\chi m \sinh[m(\tau_H + 2\chi)]} \tag{14}$$

for the interval $0 \leqslant \tau \leqslant \tau_H$. We note the symmetric roles of source (τ_0) and observation (τ) positions. This is as expected from basic reciprocity considerations since, viewed as a detector response, J in Eq. (2) models an omnidirectional instrument and the source is itself isotropic.

We now invoke the identities

$$\frac{\cosh[(b - a)m]}{\sinh[bm]} = [\exp(-am) + \exp(am - 2bm)] \times \sum_{n=0}^{\infty}\exp(-2bn) = \sum_{n=-\infty}^{\infty}\exp(-|a + 2nb|m), \quad \text{if } 0 < a < b, \tag{15a}$$

$$\exp(-ms) = \int_0^{\infty}\delta(x - s)\exp(-mx)\mathrm{d}x, \quad \text{if } s > 0. \tag{15b}$$

By performing the inverse Fourier transformation term by term of Eqs. (14) and (15) with respect to $\vec{k}$ from Eq. (10) for m, we obtain

$$J(s, \vec{\rho}, \tau) = \frac{c\sigma_e{}^3 E_0}{2\chi\pi} \times \sum_{n=-\infty}^{+\infty}\left\{\frac{\exp(-\gamma\sqrt{\rho^2 + [|\tau - \tau_0| + 2n(\tau_H + 2\chi)]^2})}{\sqrt{\rho^2 + [|\tau - \tau_0| + 2n(\tau_H + 2\chi)]^2}} - \frac{\exp(-\gamma\sqrt{\rho^2 + [(\tau + \tau_0) + 2\chi + 2n(\tau_H + 2\chi)]^2})}{\sqrt{\rho^2 + [(\tau + \tau_0) + 2\chi + 2n(\tau_H + 2\chi)]^2}}\right\}, \tag{16}$$

where

$$\gamma = [3(1 + s - \varpi_0)(1 + s - \varpi_0 g)]^{1/2}. \tag{17}$$

B. Asymptotics of the Green Function of the Diffusion Approximation

The above result provides us with an obvious exponential-like asymptotic [$\rho \gg \max(\tau, \tau_0)$] expression only in the case of a semi-infinite slab ($\tau_H \to \infty$):

$$J(s, \vec{\rho}, \tau) \sim \frac{\gamma\exp(-\gamma\rho)}{\rho^2} + \frac{\exp(-\gamma\rho)}{\rho^3}. \tag{18}$$

The second term on the right-hand side can be neglected if $\gamma \neq 0$ but becomes the main term when $\gamma = 0$. This makes the asymptotic behavior algebraic, $\sim\rho^{-3}$, in the

steady-state ($s = 0$) case with no absorption ($\varpi_0 = 1$).

If τ_H is finite, Eq. (16) cannot provide us immediately with the asymptotic behavior of $J(s, \tau, \vec{\rho})$. Moreover, numerical calculation based on this formula is complicated by the slow convergence of the series. Thus we need to change this equation to a more convenient form. The necessary transformation may be performed by use of the Poisson sum formula (Ref. 30, Sec. 4.8, p. 467)

$$\sum_{n=-\infty}^{+\infty} f(\alpha n) = \frac{1}{\alpha} \sum_{n=-\infty}^{+\infty} \tilde{f}\left(\frac{2n\pi}{\alpha}\right), \tag{19}$$

where $\alpha > 0$, $f(\cdot)$ is a square-integrable function on $(-\infty, +\infty)$, and $\tilde{f}(\cdot)$ is its Fourier transform.

First, we consider the simpler case of a steady source by setting $s = 0$ in Eqs. (16) and (17). Accordingly, we remove a factor $c\sigma$ from Eq. (16) to reflect the absence of $\delta(t)$ in relation (4a); hence, the new implicit dimensions of E_0. (It now represents a constant source in photons per second.) To make use of Eq. (19), Bateman's tables [Ref. 31, Sec. 1.4, Eq. (27)] provide us with

$$\int_{-\infty}^{\infty} \frac{\exp(-\gamma\sqrt{\rho^2 + (a + x)^2})}{\sqrt{\rho^2 + (a + x)^2}} \exp(-i\xi x)\mathrm{d}x = 2\exp(i\xi a) K_0(\rho\sqrt{\xi^2 + \gamma^2}), \tag{20}$$

where $K_0(\cdot)$ is the modified Bessel function. By setting $\alpha = 2(\tau_H + 2\chi)$ in Eq. (19), we obtain

$$J(\vec{\rho}, \tau) = E_0 \frac{2\sigma_e{}^2}{\pi\chi(\tau_H + 2\chi)} \sum_{n=1}^{\infty} \sin\left[\frac{\pi n(\tau + \chi)}{\tau_H + 2\chi}\right] \times \sin\left[\frac{\pi n(\tau_0 + \chi)}{\tau_H + 2\chi}\right] \times K_0\left\{\rho\left[\gamma^2 + \left(\frac{\pi n}{\tau_H + 2\chi}\right)^2\right]^{1/2}\right\}. \tag{21}$$

In contrast with Eq. (16) at $s = 0$, Eq. (21) provides a clear asymptotic expression at $\rho \to \infty$ for finite τ_H in the form

$$J(\vec{\rho}, \tau) \approx E_0 \frac{2\sigma_e{}^2}{\pi\chi(\tau_H + 2\chi)} \sin\left[\frac{\pi(\tau + \chi)}{\tau_H + 2\chi}\right] \sin\left[\frac{\pi(\tau_0 + \chi)}{\tau_H + 2\chi}\right] \times \left\{\frac{\pi}{2\rho\left[\gamma^2 + \left(\frac{\pi}{\tau_H + 2\chi}\right)^2\right]^{1/2}}\right\}^{1/2} \times \exp\left\{-\rho\left[\gamma^2 + \left(\frac{\pi}{\tau_H + 2\chi}\right)^2\right]^{1/2}\right\}, \tag{22}$$

hence

$$J(\vec{\rho}, \tau) \sim \frac{\exp\left\{-\rho\left[\gamma^2 + \left(\frac{\pi}{\tau_H + 2\chi}\right)^2\right]^{1/2}\right\}}{\sqrt{\rho}}. \tag{23}$$

Note that the shape of the asymptotic behavior depends only on the absorption of the medium through the diffusion constant, $\gamma(s = 0) = [3(1 - \varpi_0)(1 - \varpi_0 g)]^{1/2}$ and on how the energy drains through the lower boundary, which is determined by the slab optical thickness τ_H and the extrapolation length χ. It is interesting that neither the source depth τ_0 nor (by reciprocity) the depth τ at which the radial dependence is estimated affect the relative form of the asymptotic tail, but only the overall prefactor in relation (22). Comparing relations (18) and (23), we see that for a finite τ_H the asymptotic law is an exponential even for a nonabsorbing medium ($\gamma = 0$). Additionally, in this case the radiance density is inversely proportional to $\rho^{1/2}$, in contrast with the dependence shown in Eq. (18). As a consequence of the Poisson sum rule, the asymptotic law in the form of relation (23) does not transfer to relation (18) at $\tau_H \to \infty$ in a simple way. Analyzing Eq. (21) carefully, we can see that if $\tau_H \to \infty$, every term of the series tends to zero, and, to estimate the density at a given ρ correctly, more terms are required the larger the value of τ_H.

It is clear that relation (22) is accurate if the contribution of the first term is much greater than that of the second one. Let us make an estimation of the validity range by constructing the corresponding ratio, assuming for simplicity that $\tau_H \gg \max(2\chi, \tau, \tau_0)$ in a nonabsorbing situation $\gamma = 0$, and using the asymptotic expansion of $K_0(x)$. We obtain

$$2\sqrt{2}\exp\left[-\rho\left(\frac{\pi}{\tau_H + 2\chi}\right)\right] \ll 1, \tag{24}$$

hence

$$\rho \gtrsim \tau_H + 2\chi. \tag{25}$$

This means that relation (23) becomes accurate at radial distances exceeding the thickness of the slab by at least two extrapolation lengths. A similar analysis applied to Eq. (16) shows that the first term of this formula provides the most contribution to the reflection for the same nonabsorbing case $\gamma = 0$ if

$$\tau_H \gg \sqrt{\rho^3/8\chi}, \tag{26}$$

with a similar assumption of $\min(\rho, \tau_H) \gg \max(2\chi, \tau, \tau_0)$. Comparison of relation (25) with relation (26) shows that these conditions do not overlap, thus relations (18) and (23) have different ranges of applicability.

Relation (22) also shows that the shape of the asymptotic tail does not depend on the source depth τ_0. The DA solution for the case of a collimated illumination (e.g., a laser beam) at a boundary may be expressed through the solution for the point source by using integration over τ_0 with an exponential weight function.[13] The relative radial distribution produced by the laser beam therefore has the same asymptotic behavior as the point source at arbitrary depth. Moreover, because the net flux F_z through the slab boundaries is proportional to the radial density J (see below), any directional characteristic of the reflected radiance will also have the asymptotic behavior obtained for the internal point source.

If time dependence is of interest, we should additionally perform the inverse Laplace transformation of Eq. (16). It can be done either before or after the use of the Poisson sum formula in Eq. (19). Since we are interested in the t asymptotic, which draws on the properties of the Laplace transform at $s \to 0$,[32] we can neglect the depen-

dence of χ on s in Eq. (12) as compared to its effect through γ in Eq. (17). Since the DA is valid for the case of weakly absorbing media ($1 - \varpi_0 \ll 1$),[12,13] we may assume that

$$\gamma \underset{s\to 0}{\approx} [3(1 + s - \varpi_0)(1 - \varpi_0 g)]^{1/2}, \tag{27}$$

which leads to the known result[13]

$$J(u, \vec{\rho}, \tau) = E_0 \frac{2c\sigma_e{}^3 \exp[-(1 - \varpi_0)u]}{\tau_H + 2\chi} \frac{1}{2\pi\chi u} \times \exp\left[-\frac{\rho^2}{2\chi u}\right] \sum_{n=1}^{\infty} \sin\left[\frac{\pi n(\tau + \chi)}{\tau_H + 2\chi}\right] \times \sin\left[\frac{\pi n(\tau_0 + \chi)}{\tau_H + 2\chi}\right] \exp\left[-\frac{\chi u}{2}\left(\frac{\pi n}{\tau_H + 2\chi}\right)^2\right], \tag{28}$$

where E_0 is again equated to the total pulse energy. By integration over $\vec{\rho}$, we obtain the temporal Green function $J(u, \tau)$, which has the leading asymptotic expression for $n = 1$,

$$J(u, \tau) \sim \exp\left\{-\left[(1 - \varpi_0) + \frac{\pi^2\chi}{2(\tau_H + 2\chi)^2}\right]u\right\}, \tag{29}$$

at any depth τ. Again we see that the presence of the boundaries at finite range leads to an exponential decay, even in the absence of absorption ($\varpi_0 = 1$).

It follows from formula (28) that the instantaneous lateral distribution of radiance has a Gaussian form where the spread is proportional to nondimensional time u. This is as generally expected in the DA since, by using Eq. (6) to return to dimensional units, the argument $\rho^2/2\chi u$ of the spatial exponential term in Eq. (28) becomes $r^2/4Dt$ where D is photon diffusivity in Eq. (5). Evans *et al.*[33] obtained the case of $\tau_0 = \tau_H/2$ in Eq. (28) while investigating the feasibility of their "*in situ*" cloud lidar concept when the isotropic pulsed source and omnidirectional detector are embedded deep within the cloud. With this special choice of source position, the second since function in Eq. (28) is alternating ± 1 for odd n and 0 for even n.

3. NUMERICAL VERIFICATION

To provide verification of the results obtained above, Monte Carlo simulations were performed. This is, of course, a way of solving the radiative transfer equation, not the diffusion or telegrapher's equations used here. So we expect numerical agreement only in space-time regimes that are dominated by highly scattered photons. We emphasize light escaping from the boundaries of the optical medium at $z = 0$ ($\tau = 0$) and $z = H$ ($\tau = \tau_H$) because of its relevance to noninvasive—and even remote—observations.

The outgoing boundary flux fields in the DA look like the expressions for the (mixed) boundary conditions in Eqs. (11), but with opposite signs in the first-order derivative terms:

$$F_0(s, \vec{k}) = \frac{1}{2}\left(1 + \chi\frac{\partial}{\partial\tau}\right) J(s, \vec{k}, \tau)|_{\tau=0}, \tag{30a}$$

$$F_H(s, \vec{k}) = \frac{1}{2}\left(1 - \chi\frac{\partial}{\partial\tau}\right) J(s, \vec{k}, \tau)|_{\tau=\tau_H}. \tag{30b}$$

In the case of interest here where there is no incoming flux to account for in the boundary conditions (11) or (13), we see that the escaping fluxes are simply the photon densities at the (nonextrapolated) boundaries:

$$F_0(s, \vec{k}) = J(s, \vec{k}, 0), \tag{31a}$$

$$F_H(s, \vec{k}) = J(s, \vec{k}, \tau_H). \tag{31b}$$

All the above expressions in Fourier-Laplace space, of course, carry over to physical space–time representations. Our primary interest here is in the steady-state case, where we simply ignore the first argument and reinterpret the source strength E_0 as an injection rate.

For the DA, we can express the normalized Green function as the ratio $F_H(\vec{r})/T$. Total transmission T of the slab is the spatial integral of $F_H(\vec{r})$ [$=J(\vec{r}, H)$ in the DA], the outgoing flux at the nonilluminated boundary, for $E_0 = 1$. This is simply the "dc" component of the Fourier transform: $T = J(\vec{k} = \vec{0}, \tau = \tau_H)$. If $\varpi_0 = 1$, T will depend only on τ_H and χ and, in fact, just their ratio, which is proportional to the rescaled optical depth $(1 - g)\tau_H$. Taking into account Eqs. (1), (9a), and (14) with $E_0 = 1$, $\tau = \tau_H$, and $s = k = 0$ in Eq. (10), it can indeed be shown that

$$T = \frac{1}{1 + \tau_H/2\chi}, \tag{32}$$

while noting that a second-order Taylor expansion of Eq. (14) at $m = k = 0$ is required to remove the indeterminacy. Similarly, albedo R is the spatial integral of $F_0(\vec{r})$ [$=J(\vec{r}, 0)$ in the DA] for $E_0 = 1$. In the absence of absorption ($\sigma_s = \sigma_e$, $\varpi_0 = 1$), it follows directly from Eq. (4a) in steady state that $R + T = 1$, a global expression of radiant energy conservation. Conservative media therefore have

$$R = \frac{\tau_H/2\chi}{1 + \tau_H/2\chi} \tag{33}$$

in the DA used here.

We first consider a homogeneous slab of geometrical thickness $H = 0.3$ km and optical thickness $\tau_H = 16$ illuminated by a steady, isotropic point source at the lower boundary ($\tau_0 = 0$). The optical properties of the scattering medium are determined by the extinction coefficient $\sigma_e = 16/0.3 = 53.3\,\mathrm{km}^{-1}$, the single-scattering albedo $\varpi_0 = 1$, and the Henyey–Greenstein phase function[34] with asymmetry parameter $g = 0$ (isotropic scattering) or $g = 0.85$ (forward-biased scattering). Figure 1 contains simulation results of the normalized Green function for transmission as a function of r, the physical distance to the vertical projection of the source position onto the opposite boundary.

The normalized Green function for transmission $F_H(r)/T$ was thus calculated by using Monte Carlo meth-

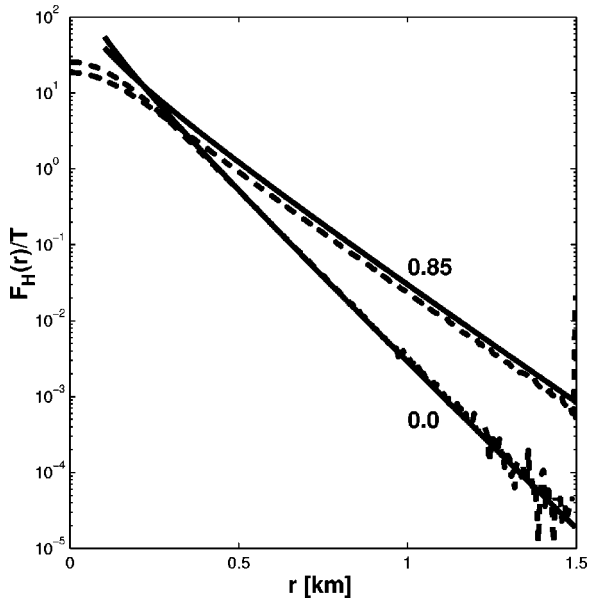

Fig. 1. Normalized flux density $F_H(r)/T$ as a function of radial distance r at the top of a slab of thickness $H = 0.3$ km for an isotropic point source at the bottom. The extinction coefficient σ_e is 53.3 km^{-1} (optical thickness $\tau_H = \sigma_e H$ is 16), the single-scattering albedo ϖ_0 is unity, and the numbers near the curves show the asymmetry parameter g of the assumed Henyey–Greenstein phase function.

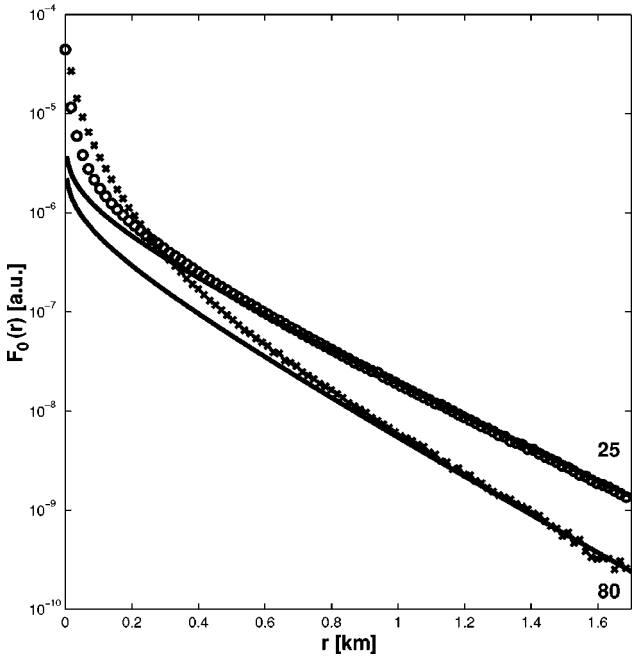

Fig. 2. Flux density $F_0(r)$ as a function of radial distance r at the bottom of the slab of thickness $H = 0.7$ km illuminated on the same boundary by a collimated beam. The curves show the results of calculations by using Eq. (34); numerical (Monte Carlo) results are depicted by symbols. The numbers near the curves are the optical thickness τ_H of the slab. The single-scattering albedo ϖ_0 is 1. Our diffusion-based expression requires the asymmetry parameter g of the Deirmendjian "Cloud.C1" phase function that we used in the Monte Carlo simulation, which is 0.85.

ods (dashed curves) and Eq. (22) (solid curves) to obtain the DA estimate $J(\vec{r}, H)/T$. The figure clearly shows that the dependence

$$J(\vec{r}, z) \sim \frac{1}{\sqrt{r}} \exp\left[-\frac{r}{r_c}\right] \tag{34}$$

obtained in the previous section for any z describes the asymptotic behavior accurately at $r > H$. This coincides roughly with our *a priori* estimation in relation (25). In the important case of a conservative media ($\varpi_0 = 1$), the predicted decay rate of the exponential tail is

$$r_c = \frac{H}{\pi}\left[1 + \frac{2\chi}{\tau_H}\right] = \frac{H}{\pi R}, \tag{35}$$

where χ is from Eq. (12) and R is from Eq. (33).

Simulations were also made for a cloud with a more realistic "Cloud C.1"-type phase function[35] being illuminated by a collimated beam, as in real laser probing. The geometrical thickness H of the cloud is 0.7 km and its optical thickness τ_H is 25 or 80. The radial distribution of the flux density has been computed employing the asymptotic formula (shown by solid curves in Fig. 2) and by Monte Carlo simulation (depicted by symbols), in this case for reflection ($z = z_0 = 0$). The asymptotic results have been multiplied by a factor of 0.83. This is consistent with the level of uncertainty in χ that is present in the complicated prefactor of the exponential term in relation (22). The figure shows that the shape of the asymptotic tail can also be successfully described by relation (34) in the case of illumination by a collimated (laser-like) beam.

Finally, if we rewrite relation (29) with $\varpi_0 = 1$ as

$$J(t, z) \sim \exp[-t/t_c], \tag{36}$$

this defines the characteristic time scale t_c. By using Eqs. (6), (12), (29), and (35), we find the relation

$$t_c = \frac{2}{\pi^2}\left(\frac{H}{c}\right)\frac{\tau_H}{\chi R^2} = \frac{3(1-g)\sigma_e}{c} r_c{}^2. \tag{37}$$

Comparing with Eq. (5), we can see that $r_c{}^2/t_c = D$. However, this is only true if the numerator in the definition of the extrapolation length χ in Eq. (12) is indeed 2/3 in the expression of boundary conditions in Eqs. (11) or (13). Yet we know this is not always the best value to use, so we can only expect $r_c{}^2/t_c \approx D$, and a similar qualification follows for Eq. (37), with the theoretical correction factor being $(3\chi/2)$. Therefore, if we compare the r_c and t_c as potential diagnostics of media with some optical or geometrical properties unknown, the presence of $1/\chi$ as a multiplicative factor in Eq. (37) is a disadvantage over the simpler result in Eq. (35) where χ appears only as an additive term in R^{-1}.

4. EFFECT ON CLOUD REMOTE SENSING AND OPTICAL DIAGNOSTICS

In the case of clouds, at least, albedo R is relatively easy to measure directly with a calibrated radiometer, but it is not so easily converted into an estimate of optical thickness τ_H.[36] In sharp contrast, H is generally unknown for

clouds even though it is a highly desirable quantity in climate and weather studies. Thus, combined with R, empirical estimates of r_c in Eq. (35) can be used to infer H. If the Green function is not immediately available to evaluate r_c using a laser source, then it can be obtained indirectly from the wave number spectrum of the fluctuations of cloud radiance from reflected[26] or transmitted[37] sunlight. Indeed, these fluctuations can be represented as a convolution of the cloud's internal turbulent structure (a "$k^{-5/3}$" spectrum) with a smoothing kernel that can be taken as the simple expression in relation (34).[38]

It is interesting to compare our steady-state asymptotics in relations (34) and (35) with how Marshak *et al.*[36] empirically parameterized their Monte Carlo estimations of transmitted and reflected Green functions with Gamma-type distributions $r^{\alpha-2}\exp[-\alpha(r/\eta)]$ where α and η are free parameters determined from the first and second moments of r: $\eta = \langle r\rangle$ and $1/\alpha + 1 = \langle r^2\rangle/\langle r\rangle^2$. Their results for α, of course, capture the near-field tendencies better than our universal far-field value of 3/2: 2+ in transmission (see Fig. 1) and $\approx$1/2 in reflection (see Fig. 2). However, their estimates of $r_c = \eta/\alpha$ are reasonably close ($\pm$20%) to our result from formula (35) for the one homogeneous cloud case (their Fig. 7) where there is enough information to make a prediction. In view of the emphasis given to small and intermediate values of r by the moment-based parameter estimation technique, we consider this very good agreement.

Our analytical diffusion theoretic expressions for the Green functions may have a direct application in the follow-on study by Marshak *et al.*,[38] where the convenient but *ad hoc* Gamma model is used to improve cloud remote sensing in the solar spectrum at pixel scales where 3D radiative transfer effects blur our satellite retrievals.[26,36] This study uses one-dimensional radiative transfer in each pixel (i.e., vertical column in cloud layer) as a first guess for the radiance escaping from the boundary of the three-dimensional medium—this is the independent pixel approximation or "IPA"[25]—and then improves it by convolution with the appropriate Green function. Marshak *et al.* call this the nonlocal IPA or NIPA and show that the precise choices for α and η were not critical as long as their values capture the near- and far-field trends, respectively. In Fourier space, α controls the ultimate decay as wave number increases without bound while η (our r_c) controls the onset of radiative smoothing.

In the spirit of the NIPA, Polonsky, Box, and Davis have recently computed perturbations in the radiance field caused by deviations from strict spatial uniformity at the first[39] and then at higher[40] orders. The Green function plays a central role in perturbation theory so the analytic results obtained in Section 2 for the DA will also find application in that efficient computational framework for 3D radiative transfer. How much NIPA-like or perturbative techniques can enhance the inference of internal structure with noninvasive optical diagnostics for biological tissues remains to de determined.

5. CONCLUSIONS AND OUTLOOK

We have used the diffusion approximation to estimate the asymptotic behavior of the radiance propagating in optically thick, weakly absorbing slab media. Relation (23) provides the dependence of the mean radiance density on the radial distance. A comparison with Monte Carlo simulations show that this asymptotic dependence is accurate for pure scattering. This formula was derived for the case of a point source, although it follows from our diffusion theory that the same asymptotic behavior will be observed either for the case of a directed source, such as a laser beam, or for the measurement of the directed characteristics of the reflected or transmitted radiance. Comparison with Monte Carlo results confirms this prediction.

The difference in the asymptotic behavior for a semi-infinite medium and for a finite slab is discussed, which leads to the conclusion that the use of the radial asymptotic obtained in the case of the semi-infinite slab to analyze real measurements on finite systems should be performed with extreme care. The effect of the additional boundary is not limited to the appearance of extra absorption in the exponential term: the radial dependence is also inversely proportional to the square root of the distance to the beam. This is also confirmed by Monte Carlo simulation and is completely different from the prediction of the semi-infinite slab theory.

One direction of further investigation is to use our new insights into Green function theory to develop an approximate but efficient approach to 3D radiative transfer in spatially heterogeneous optical media. Examples that come to mind are clouds and soft tissue with embedded anomalies. First steps have already been taken along this path that use homogeneous media as a baseline and exploit the 3D radiative transfer information contained in the Green function.[39,40] Conversely, we are also interested in how sensitive the asymptotic law obtained here is to deviations of the scattering medium's optical properties from uniformity. Here again we will use the perturbation technique suggested by Marchuk[41] and generalized by Polonsky and Box.[42] Finally, we will apply our results to the analysis of wide-angle imaging lidar (WAIL) data collected during a validation campaign where a wide variety of cloud-probing instruments were operating simultaneously.[43]

ACKNOWLEDGMENTS

This research was supported by the Office of Biological and Environmental Research of the U.S. Department of Energy as part of the Atmospheric Radiation Measurement Program. We thank Luc Bissonnette, Robert Cahalan, James Spinhirne, David Winker, and Eleonora Zege for fruitful discussions leading to this paper.

Corresponding author I. N. Polonsky's e-mail address is polonsky@lanl.gov.

REFERENCES

1. B. N. Holben, T. I. Eck, I. Slutsker, D. Tar, J. P. Buis, A. Setxer, J. E. Vemte, J. A. Reagan, K. Y. J. T. Nakajima, F. Lavenu, I. Jankowiak, and A. Smirnov, "AERONET–A federated instrument network and data archive for aerosol characterization," Remote Sens. Environ. **66**, 1–16 (1998).
2. M. Patterson, J. Moulton, and B. Wilson, "Time-resolved reflectance and transmittance for the noninvasive measure-

ment of tissue optical properties," Appl. Opt. **28**, 2331–2336 (1989).
3. S. R. Arridge, M. Cope, and D. T. Delpy, "The theoretical basis for the determination of optical pathlengths in tissue: Temporal and frequency analysis," Phys. Med. Biol. **37**, 1531–1560 (1992).
4. A. Kienle and M. S. Patterson, "Improved solutions of the steady-state and the time-resolved diffusion equations for reflectance from a semi-infinite turbid medium," J. Opt. Soc. Am. A **14**, 246–254 (1997).
5. D. Contini, F. Martelli, and G. Zaccanti, "Photon migration through a turbid slab described by a model based on diffusion approximation. I. Theory," Appl. Opt. **36**, 4587–4599 (1997).
6. A. B. Davis, R. F. Cahalan, J. D. Spinhirne, M. J. McGill, and S. P. Love, "Off-beam lidar: An emerging technique in cloud remote sensing based on radiative Green-function theory in the diffusion domain," Phys. Chem. Earth **24**, 757–765 (1999).
7. A. B. Davis and A. Marshak, "Space–time characteristics of light transmitted by dense clouds. A Green function analysis," J. Atmos. Sci. **59**, 2713–2727 (2002).
8. H. Gordon, "Interpretation of airborne oceanic lidar: Effects of multiple scattering," Appl. Opt. **21**, 2996–3001 (1982).
9. H. Gordon and A. Morel, *Remote Assessment of Ocean Color for Interpretation of Satellite Visible Imagery*, Vol. 4 of Lecture Notes on Coastal and Estuarine Studies (Springer-Verlag, New York, 1983).
10. S. Chandrasekhar, *Radiative Transfer* (Oxford U. Press, London, 1950).
11. A. Ishimaru, *Wave Propagation and Scattering in Random Media* (Academic, New York, 1978).
12. B. Davison, *Neutron Transport Theory* (Clarendon, Oxford, UK, 1957).
13. E. Zege, A. Ivanov, and I. Katsev, *Image Transfer Through a Scattering Medium* (Springer-Verlag, Heidelberg, Germany, 1991).
14. J. Li, J. Geldart, and P. Chylek, "Perturbation solution for 3D radiative transfer in a horizontally periodic inhomogeneous cloud field," J. Atmos. Sci. **51**, 2110–2122 (1994).
15. A. Davis and A. Marshak, "Multiple scattering in clouds: Insights from three-dimensional diffusion/P_1 theory," Nucl. Sci. Eng. **137**, 251–280 (2001).
16. T. Farrel, M. Patterson, and M. Essenpreis, "Influence of layered tissue architecture on estimates of tissue optical properties obtained from spatially resolved diffuse reflectometry," Appl. Opt. **37**, 1958–1972 (1998).
17. J. Hampel, E. Schleicher, and R. Freyer, "Volume image reconstruction for diffuse optical tomography," Appl. Opt. **41**, 3816–3826 (2002).
18. M. Ostermeyer and S. Jacques, "Perturbation theory for diffuse light transport in complex biological tissues," J. Opt. Soc. Am. A **14**, 255–261 (1997).
19. S. P. Love, A. B. Davis, C. Ho, and C. A. Rohde, "Remote sensing of cloud thickness and liquid water content with Wide-Angle Imaging Lidar (WAIL)," Atmos. Res. **59–60**, 295–312 (2001).
20. P. I. Richards, "Scattering from a point-source in plane clouds," J. Opt. Soc. Am. **46**, 927–934 (1956).
21. J.-M. Tualle, B. Gélébart, E. Tinet, S. Avrillier, and J.-P. Ollivier, "Real time optical coefficients evaluation from time and space resolved reflectance measurements in biological tissues," Opt. Commun. **124**, 216–221 (1996).
22. R. M. P. Doornbos, R. Lang, M. C. Aalders, F. W. Cross, and H. J. C. M. Sterenborg, "The determination of *in vivo* human tissue optical properties and absolute chromophore concentrations using spatially resolved steady-state diffuse reflectance spectroscopy," Phys. Med. Biol. **44**, 967–981 (1999).
23. S. Stolik, J. A. Delgado, A. Perez, and L. Anasagasti, "Measurement of the penetration depths of red and near infrared light in human "*ex vivo*" tissues," J. Photochem. Photobiol. B **57**, 90–93 (2000).
24. A. A. Kokhanovsky and E. P. Zege, "On remote sensing of water clouds from space," Adv. Space Res. **21**, 425–428 (1998).
25. R. F. Cahalan, W. Ridgway, W. J. Wiscombe, S. Gollmer, and Harshvardhan, "Independent pixel and Monte Carlo estimates of stratocumulus albedo," J. Atmos. Sci. **51**, 3776–3790 (1994).
26. A. Davis, A. Marshak, R. F. Cahalan, and W. J. Wiscombe, "The Landsat scale-break in stratocumulus as a three-dimensional radiative transfer effect: Implications for cloud remote sensing," J. Atmos. Sci. **54**, 241–260 (1997).
27. B. D. Ganapol, D. E. Kornreich, J. A. Dahl, D. W. Nigg, S. N. Jahshan, and C. A. Temple, "The searchlight problem for neutrons in a semi-infinite medium," Nucl. Sci. Eng. **118**, 38–53 (1994).
28. L. M. Romanova, "Narrow light beam propagation in a stratified cloud: Higher transverse moments," Izv., Acad. Sci., USSR Atmos. Oceanic Phys. **37**, 748–756 (2001).
29. G. C. Pomraning, "Diffusion theory via asymptotics," Transp. Theory Stat. Phys. **18**, 383–428 (1989).
30. P. Morse and H. Feshbach, *Methods of Theoretical Physics* (McGraw-Hill, New York, 1952).
31. A. Erdelyi, ed., *Tables of Integral Transforms*, Vol. 1 (McGraw-Hill, New York, 1954).
32. G. Doetsch, *Guide to the Application of the Laplace and Z-Transforms* (Van Nostrand Reinhold, New York, 1971).
33. K. F. Evans, R. P. Lawson, P. Zmarzly, D. O'Connor, and W. J. Wiscombe, "*In situ* cloud sensing with multiple scattering lidar: Simulations and demonstration," J. Atmos. Oceanic Technol. **20**, 1505–1522 (2003).
34. L. Henyey and J. Greenstein, "Diffuse radiation in the galaxy," Astrophys. J. **93**, 70–83 (1941).
35. D. Deirmendjian, *Electromagnetic Scattering on Spherical Polydispersions* (American Elsevier, New York, 1969).
36. A. Marshak, A. Davis, W. J. Wiscombe, and R. F. Cahalan, "Radiative smoothing in fractal clouds," J. Geophys. Res. **100**, 26247–26261 (1995).
37. C. von Savigny, A. B. Davis, O. Funk, and K. Pfeilsticker, "Time-series of zenith radiance and surface flux under cloudy skies: radiative smoothing, optical thickness retrievals and large-scale stationarity," Geophys. Res. Lett. **29**, 1825–1828 (2002).
38. A. Marshak, A. Davis, R. F. Cahalan, and W. J. Wiscombe, "Nonlocal independent pixel approximation: direct and inverse problems," IEEE Trans. Geosci. Remote Sens. **36**, 192–205 (1998).
39. I. N. Polonsky, M. A. Box, and A. B. Davis, "Radiative transfer through inhomogeneous turbid media: implementation of the adjoint perturbation approach at the first order," J. Quant. Spectrosc. Radiat. Transf. **78**, 85–98 (2003).
40. M. A. Box, I. N. Polonsky, and A. B. Davis, "Higher-order perturbation theory applied to radiative transfer in non-plane-parallel media," J. Quant. Spectrosc. Radiat. Transf. **78**, 105–118 (2003).
41. G. Marchuk, "Equation for the value of information from weather satellite and formulation of inverse problems," Kosm. Issled. **2**, 462–477 (1964).
42. I. N. Polonsky and M. A. Box, "General perturbation technique for the calculation of radiative effects in scattering and absorbing media," J. Opt. Soc. Am. A **19**, 2281–2292 (2002).
43. S. P. Love, A. B. Davis, C. A. Rohde, L. Tellier, and C. Ho, "Active probing of cloud multiple scattering, optical depth, vertical thickness, and liquid water content using Wide-Angle Imaging Lidar," in *Atmospheric Radiation Measurements and Applications in Climate*, J. A. Show, ed., Proc. SPIE **4815**, 129–138 (2002).